



Facile synthesis of novel cobalt particles by reduction method and their microwave absorption properties

Shulai Wen, Ying Liu^{*}, Xiuchen Zhao, Jingwei Cheng, Hong Li

School of Materials Science and Engineering, Beijing Institute of Technology, Beijing 100081, People's Republic of China

ARTICLE INFO

Article history:

Received 9 January 2014

Received in revised form 12 May 2014

Accepted 17 May 2014

Available online 24 May 2014

Keywords:

Cobalt particles

Permeability

Permittivity

Reflection loss

ABSTRACT

Three kinds of cobalt particles with different morphologies and crystal structures were synthesized via reducing cobaltous sulfate ($\text{CoSO}_4 \cdot 7\text{H}_2\text{O}$) by hydrazine hydrate ($\text{N}_2\text{H}_4 \cdot \text{H}_2\text{O}$) under ultrasonic wave, in which seignette salt ($\text{C}_4\text{H}_4\text{KNaO}_6 \cdot 4\text{H}_2\text{O}$) or $\text{C}_6\text{O}_7\text{H}_5\text{Na}_3 \cdot 2\text{H}_2\text{O}$ acted as complexing agent, $\text{C}_{16}\text{H}_{33}(\text{CH}_3)_3\text{NBr}$ acted as surfactant agent and sodium hydroxide (NaOH) acted as pH regulator. Less saturation magnetization and more coercivity were obtained compared to single hcp-cobalt and bulk cobalt, respectively. The electromagnetic properties of cobalt particles dispersed in paraffin (70 wt.%) were measured in the microwave frequency range of 1–18 GHz. The three kinds of cobalt particles all have multi-nonlinear dielectric resonances due to atomic and electronic polarization. The cobalt particles composed by nanosheets exhibit higher real part of permeability in the range of 10–18 GHz compared to spherical cobalt particles. The reflection loss values of cobalt particles were calculated according to the transmission-line theory, and the minimal reflection loss of -19.06 dB at 17.42 GHz was observed corresponding to a thickness of 5 mm.

© 2014 Elsevier B.V. All rights reserved.

1. Introduction

Magnetic materials have been widely investigated to eliminate the serious electromagnetic interference problems recently. For the ferromagnetic metal particles, large values of permeability can be obtained in GHz range due to the Snoek's limit, because their saturation magnetization is higher than ferrites, such as FeCo nanoparticles [1], hexagonal Fe microflakes [2], Fe nanotubes [3], and hierarchical dendrite-like Fe [4]. As a typical magnetic metal, the electromagnetic and microwave properties of cobalt particles have been investigated in recent years. Wang et al. [5] reported that at thickness of 2 mm, flower-like cobalt with sharp petals possessed the maximum reflection loss of -13.6 dB. Tong et al. [6] found that flower-like cobalt superstructures showed excellent microwave absorption performances, with a minimum reflection loss of -40 dB, corresponding to a matching thickness of 2.5 mm. It is well-known that the electromagnetic microwave absorption properties of the cobalt particles depend on their morphologies and crystal structure, so present research is focused on their synthesis of cobalt particles with specific morphologies and crystal structure. Cobalt particles possess three crystal structures (FCC, HCP and BCC) [7] and various morphologies, such as hollow cobalt mesospheres [8], ring-shaped cobalt nanomaterials [9], cobalt tubes [10,11], cobalt rods [12,13], and cobalt wires [14–17]. However, few investigations have been focus on dependence of electromagnetic and microwave properties on the crystal structures and morphologies of cobalt particles. It is valuable to

obtain excellent electromagnetic microwave absorption via adjusting the crystal structures and morphologies of cobalt particles.

In the present paper, three kinds of cobalt particles, with nanosheets, porous surface and smooth surface, were successfully synthesized by facile reduction method via reducing cobaltous sulfate ($\text{CoSO}_4 \cdot 7\text{H}_2\text{O}$) by hydrazine hydrate ($\text{N}_2\text{H}_4 \cdot \text{H}_2\text{O}$) under ultrasonic wave, in which seignette salt ($\text{C}_4\text{H}_4\text{KNaO}_6 \cdot 4\text{H}_2\text{O}$) or $\text{C}_6\text{O}_7\text{H}_5\text{Na}_3 \cdot 2\text{H}_2\text{O}$ acted as complexing agent, $\text{C}_{16}\text{H}_{33}(\text{CH}_3)_3\text{NBr}$ acted as surfactant agent and sodium hydroxide (NaOH) acted as pH regulator. We investigated the electromagnetic and microwave properties of cobalt particles dispersed in paraffin (70 wt.%) in detail. The three kinds of cobalt particles all have multi-nonlinear dielectric resonances due to atomic and electronic polarization. The cobalt particles composed by nanosheets exhibit higher real part of permeability in the microwave frequency range of 10–18 GHz compared to spherical cobalt particles. The high yields, simple instrument and mild conditions would make the method good prospect in future large-scale applications.

2. Experimental

2.1. Preparation of cobalt particles

Cobaltous sulfate ($\text{CoSO}_4 \cdot 7\text{H}_2\text{O}$), seignette salt ($\text{C}_4\text{O}_6\text{H}_4\text{KNa} \cdot 4\text{H}_2\text{O}$), sodium citrate ($\text{C}_6\text{O}_7\text{H}_5\text{Na}_3 \cdot 2\text{H}_2\text{O}$), hydrazine hydrate ($\text{N}_2\text{H}_4 \cdot \text{H}_2\text{O}$), cetyl trimethyl ammonium bromide ($\text{C}_{16}\text{H}_{33}(\text{CH}_3)_3\text{NBr}$) and sodium hydroxide (NaOH) were purchased from Beijing Tongguangxincheng Co. Ltd. All chemicals used in this work were of analytical grade and were used as received without further purification. The synthesis of

^{*} Corresponding author.

E-mail addresses: zhaoxiuchen@bit.edu.cn, abc.1984816@163.com (Y. Liu).

cobalt particles was carried out in a 3-necked flask equipped with an ultrasound reactor. The three kinds of cobalt particles, S1, S2 and S3, were processed as follows:

For S1, 2.8 g $\text{CoSO}_4 \cdot 7\text{H}_2\text{O}$, 1 g $\text{C}_{16}\text{H}_{33}(\text{CH}_3)_3\text{NBr}$ (C_{16}TAB) and 12.6 g $\text{C}_6\text{O}_7\text{H}_5\text{Na}_3 \cdot 2\text{H}_2\text{O}$ were dissolved in 150 mL deionized water under vigorous stirring for 40 min at 40 °C, followed by 4 g NaOH. The reaction temperature, the power and the ultrasonic frequency were fixed at 90 °C, 1400 W and 40 kHz, respectively. After that, 0.5 mL $\text{N}_2\text{H}_4 \cdot \text{H}_2\text{O}$ (80 wt.%) was quickly added to the above solution, then 10 min later, the solution was cooled to room temperature. The dark gray precipitates were separated, washed with deionized water and absolute ethanol several times, and dried under vacuum at 40 °C for 24 h to collect the cobalt particles.

For S2, 1.4 g $\text{CoSO}_4 \cdot 7\text{H}_2\text{O}$, 1 g $\text{C}_{16}\text{H}_{33}(\text{CH}_3)_3\text{NBr}$ (C_{16}TAB) and 8.4 g $\text{C}_4\text{O}_6\text{H}_4\text{KNa} \cdot 4\text{H}_2\text{O}$ were dissolved in 150 mL deionized water under vigorous stirring for 40 min at 40 °C, followed by 14 g NaOH. Then the reaction temperature, the power and the ultrasonic frequency were fixed at 65 °C, 1400 W and 40 kHz, respectively. After that, 0.5 mL $\text{N}_2\text{H}_4 \cdot \text{H}_2\text{O}$ (80 wt.%) was quickly added to the above solution, and 10 min later, the solution was cooled to room temperature. The dark gray precipitates were separated, washed with deionized water and absolute ethanol several times, and dried under vacuum at 40 °C for 24 h to collect the cobalt particles. For S3, 2.8 g $\text{CoSO}_4 \cdot 7\text{H}_2\text{O}$, 4 g $\text{C}_{16}\text{H}_{33}(\text{CH}_3)_3\text{NBr}$ (C_{16}TAB) and 12.6 g $\text{C}_4\text{O}_6\text{H}_4\text{KNa} \cdot 4\text{H}_2\text{O}$ were dissolved in 150 mL deionized water under vigorous stirring for 40 min at 40 °C, followed by 14 g NaOH. Then the reaction temperature, the power and the ultrasonic frequency were fixed at 90 °C, 1400 W and 40 kHz, respectively. After that, 1.3 mL $\text{N}_2\text{H}_4 \cdot \text{H}_2\text{O}$ (80 wt.%) was quickly added to the above solution, and 10 min later, the solution was cooled to room temperature. The dark gray precipitates were separated, washed with deionized water and absolute ethanol several times, and dried under vacuum at 40 °C for 24 h to collect the cobalt particles.

2.2. Instruments and measurements

The X-ray diffraction (XRD) patterns were recorded on a Bruker D8 Advance diffractometer in Mo K_α radiation ($\lambda = 0.7093 \text{ \AA}$) operated at 50 kV and 30 mA. The scanning electron microscopy (SEM) images were obtained using a QUANTA600 scanning electron microscope operated at 25 kV. The magnetization measurement was performed by a DMS vibrating sample magnetometer (VSM) at room temperature. The relative complex permittivity ($\epsilon_r = \epsilon' - j\epsilon''$) and relative complex permeability ($\mu_r = \mu' - j\mu''$) were determined using the T/R coaxial line method in the range of 2–18 GHz with an O-ring shaped sample (i.d. = 3 mm and o.d. = 7 mm, thickness = 2 mm) using an HP8722ESS vector network analyzer. All measurements were performed at room temperature.

3. Results and discussion

The crystal structure and phase purity of the as-synthesized samples were determined by XRD. Fig. 1 shows the typical X-ray diffraction patterns of S1, S2 and S3. For S1, the characteristic peaks at $2\theta = 18.856^\circ$, 20.193° , 21.402° , 32.911° , 35.957° and 38.865° can be well indexed to the (100), (002), (101), (110), (103) and (112) planes of hexagonal-phase cobalt (space group: $P6_3/mmc$ (194); JCPDS card: 05-0727, $a = 2.503 \text{ \AA}$, $c = 4.0621 \text{ \AA}$), so S1 is hcp-cobalt structure. The peaks of S2 and S3 at $2\theta = 18.856^\circ$, 21.402° and 35.957° match very well with the (100), (101) and (103) planes of hcp-cobalt (space group: $P6_3/mmc$ (194); JCPDS card: 05-0727, $a = 2.503 \text{ \AA}$, $c = 4.0621 \text{ \AA}$), respectively, and the peaks at $2\theta = 19.957^\circ$, 32.878° , and 38.759° can be well

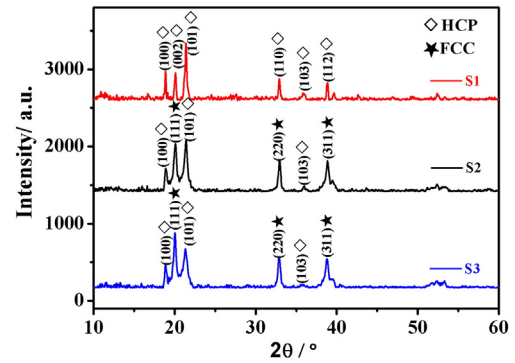


Fig. 1. The XRD patterns of the as-prepared samples.

indexed to the (111), (220) and (311) planes of fcc-cobalt (space group: $Fm\bar{3}m$ (225); JCPDS card: 15-0806, $a = 3.545 \text{ \AA}$), respectively. Due to several fcc-cobalt peaks overlapping with hcp-cobalt peaks, the structures of samples are distinguished by the relative intensity. The above result shows that S1 and S2 are mixture of fcc-cobalt and hcp-cobalt, respectively.

Fig. 2 shows the SEM images of cobalt particles. Cobalt particles with a diameter of about 5 μm were obtained (S1). The cobalt particles were assembled by nanosheets with a thickness of about 200 nm. S2 particles are spherical cobalt particles with porous surface, and the diameter is about 6 μm . S3 particles are spherical cobalt particles with smooth surface, and the size is about 7 μm .

The magnetic property of the cobalt particles is manifested in the M–H loop acquired by VSM measurement, as shown in Fig. 3. The saturation magnetization (M_s) values of S1, S2 and S3 are 90.559, 117.50 and 123.00 emu/g, respectively. The coercivity values of S1, S2 and S3 are 176.67, 190.89 and 156.80 Oe, respectively. Less saturation magnetization was achieved compared to the hcp-Co single crystal (162 emu/g) [18]. This may be attributed to the effective Bohr magneton number reduced due to the pinning effect of the ions or atom absorbed on the surface of flow-like cobalt particles, such as $[\text{C}_4\text{H}_4\text{O}_6]^{2-}$ and oxygen atom. Moreover, as-obtained cobalt particles exhibit larger coercivity compared to bulk cobalt (10 Oe) [19,20], and there may be three reasons: firstly, according to the faning mode [21,22], H_c is inversely proportional to R^3 , so H_c of cobalt particles is larger because cobalt particles are in micron scale; secondly, hcp-cobalt possesses larger magnetocrystalline anisotropy energy, which would enhance coercivity of cobalt particles; thirdly, it is well known that coercivity is related to magnetic domain and magnetic moment, and the interface between hcp-cobalt and fcc-cobalt can improve the difficulty of movement of magnetic domain and rotation of magnetic moment. The coercivity of S1, S2 and S3 are larger than that of bulk cobalt crystal, respectively.

The frequency dependency of the complex permittivity ($\epsilon_r = \epsilon' - j\epsilon''$) and complex permeability ($\mu_r = \mu' - j\mu''$) for cobalt particles–paraffin composites are shown in Fig. 4. For S3, the real part of permittivity is larger than that for S1 and smaller than that for S2 (Fig. 4a). The phenomenon can be explained on the basis of space charge polarization model of Wagner [23] and Maxwell [24] and is in agreement with the Koop's phenomenological theory. According to the Koop's model, complex permittivity behaviors are attributed to the interfacial space-charge polarization arising from the heterogeneous structure of the samples. Cobalt particles dispersed in paraffin can act as charge centers, and the interfacial space-charge polarization would appear due to charges' motion hindered in these interfaces differently when charges in cobalt are made to move by the external electric field. For S1, there is only one kind of interface: cobalt particle and paraffin. For S2 and S3, there are two kinds of interfaces: cobalt particle and paraffin and fcc-cobalt and hcp-cobalt, composed by two crystal structures, respectively. Moreover, S2 has more surface than

Download English Version:

<https://daneshyari.com/en/article/6677319>

Download Persian Version:

<https://daneshyari.com/article/6677319>

[Daneshyari.com](https://daneshyari.com)